AIAA JOURNAL
Vol. 45, No. 2, February 2007

Technical Notes

TECHNICAL NOTES are short manuscripts describing new developments or important results of a preliminary nature. These Notes should not exceed 2500 words (where a figure or table counts as 200 words). Following informal review by the Editors, they may be published within a few months of the date of receipt. Style requirements are the same as for regular contributions (see inside back cover).

Nonlinear Dynamic Thermal Buckling of Functionally Graded Spherical Caps

T. Prakash* and Maloy K. Singha†
Indian Institute of Technology, Delhi, New Delhi 110 016, India
and
M. Ganapathi‡
Institute of Armament Technology, Girinagar, Pune 411 025, India

DOI: 10.2514/1.21578

I. Introduction

RECENT research works on improved performance materials have addressed new materials, known as functionally graded materials [1](FGMs), in which the material properties vary smoothly and continuously from one surface of the material to the other surface. These are high-performance, heat-resistant materials that are able to withstand the ultrahigh temperatures and extremely large thermal gradients that are used in fusion reactors and aerospace industries. They maintain their structural integrity and avoid the interface problem that exists in homogeneous composites. Thin-walled structural members of aerospace and defense that are subjected to dynamic load could encounter deflections of the order of the shell thickness. The dynamic response of such shells may lead to the phenomenon of dynamic snapping or dynamic buckling. Hence, the nonlinear behavior of thin structural members, in particular, spherical shells that form an important class of structural components, has to be understood for their optimum design.

The investigation of such phenomenon that considers externally applied pressure load has received considerable attention in the literature: Budiansky and Roth [2] employed the Galerkin method, Simitses [3] adopted the Ritz–Galerkin procedure, and Haung [4] solved using finite difference scheme. Limited studies are also available on dynamic buckling of orthotropic shallow spherical shells [5,6]. It is further observed that similar available studies that consider thermal impact are rather meager in the literature. The studies pertaining to FGM shell structures are mainly limited to thermal stress, deformation, and static analysis in the literature [7–9]. Work on vibration/dynamic stability of FGM shell structures is also reported in the work of Ng et al. [10]. The vibration and parametric instability analysis of functionally graded cylindrical shells under harmonic axial loading have been carried out in [10,11]. However, to the authors' knowledge, work on the dynamic buckling behavior of isotropic/orthotropic/functionally graded material spherical shells suddenly exposed to thermal environment is rather meager in the literature and such studies are important to the structural designers.

In the present work, the nonlinear dynamic thermal buckling of functionally graded spherical caps is investigated using a three-noded shear flexible axisymmetric curved shell element based on field-consistency principle [6]. Geometric nonlinearity is assumed in the present study, using von Karman's strain-displacement relations. In addition, the formulation includes in-plane and rotary inertia effects. The material properties are graded in the thickness direction according to the power-law distribution in terms of volume fractions of the constituents of the material. The nonlinear governing equations derived are solved employing Newmark's numerical integration method in conjunction with the modified Newton–Raphson iteration scheme. The critical dynamic buckling temperature difference is taken as the temperature difference between the shell surfaces corresponding to a sudden jump in the maximum average displacement in the time history [2,12]. Numerical results are presented that consider different values of geometrical parameter and power-law index.

II. Formulation

An axisymmetric functionally graded shell of revolution (radius a, thickness h) made of a mixture of ceramics and metals is considered with the coordinates s, θ, and z along the meridional, circumferential, and radial/thickness directions, respectively. The materials in the outer ($z = h/2$) and inner ($z = -h/2$) surfaces of the spherical shell are ceramic and metal, respectively. The locally effective material properties are evaluated using a homogenization method that is based on the Mori–Tanaka scheme [13,14]. The effective bulk modulus K and shear modulus G of the functionally gradient material evaluated using the Mori–Tanaka estimates [13–15] are given as

$$\frac{K-K_m}{K_c-K_m} = V_c \Big/ \left[1+(1-V_c)\frac{3(K_c-K_m)}{3K_m+4G_m}\right]$$
$$\frac{G-G_m}{G_c-G_m} = V_c \Big/ \left[1+(1-V_c)\frac{(G_c-G_m)}{G_m+f_1}\right] \tag{1}$$

where

$$f_1 = \frac{G_m(9K_m+8G_m)}{6(K_m+2G_m)}$$

V is the volume fraction of the phase material, and the subscripts m and c refer to the ceramic and metal phases, respectively. The volume fractions of ceramic and metal phases are related by $V_c + V_m = 1$, and V_c is expressed as

$$V_c(z) = \left(\frac{2z+h}{2h}\right)^k \tag{2}$$

where k is the volume fraction exponent ($k \geq 0$).

The effective values of Young's modulus E and Poisson's ratio υ can be found from

$$E(z) = \frac{9KG}{3K+G} \quad \text{and} \quad \upsilon(z) = \frac{3K-2G}{2(3K+G)} \tag{3}$$

The locally effective heat conductivity coefficient κ is given as

$$\frac{\kappa-\kappa_m}{\kappa_c-\kappa_m} = V_c \Big/ \left[1+(1-V_c)\frac{(\kappa_c-\kappa_m)}{3\kappa_m}\right] \tag{4}$$

Received 5 December 2005; revision received 20 September 2006; accepted for publication 5 October 2006.

*Research Scholar, Department of Applied Mechanics.
†Assistant Professor, Department of Applied Mechanics.
‡Professor; mganapathi@hotmail.com.

The coefficient of thermal expansion α is determined in terms of the correspondence relation:

$$\frac{\alpha-\alpha_m}{\alpha_c-\alpha_m}=\left(\frac{1}{K}-\frac{1}{K_m}\right)\Big/\left(\frac{1}{K_c}-\frac{1}{K_m}\right) \tag{5}$$

The effective mass density ρ can be given by the rule of mixture as

$$\rho(z)=\rho_c V_c+\rho_m V_m \tag{6}$$

The temperature variation is assumed to occur in the thickness direction only, and the temperature field is considered constant in the x–y plane. In such a case, the temperature distribution along the thickness can be obtained by solving a steady-state heat transfer equation:

$$-\frac{d}{\mathrm{d}z}\left[\kappa(z)\frac{\mathrm{d}T}{\mathrm{d}z}\right]=0, \qquad T=T_c \quad \text{at } z=h/2$$
$$T=T_m \quad \text{at } z=-h/2 \tag{7}$$

The solution of this boundary-value problem provides the temperature distribution through the thickness of the plate.

By using the Mindlin formulation, the displacements at a point (s,θ,z) are expressed as functions of the midplane displacements u_o, v_o, and w, and independent rotations β_s and β_θ of the radial and hoop sections, respectively, as

$$u(s,\theta,z,t)=u_o(s,\theta,t)+z\beta_s(s,\theta,t)$$
$$v(s,\theta,z,t)=v_o(s,\theta,t)+z\beta_\theta(s,\theta,t) \qquad w(s,\theta,z,t)=w(s,\theta,t) \tag{8}$$

where t is the time.

Using von Karman's assumption for moderately large deformation, Green's strains can be written in terms of middle surface deformations:

$$\{\varepsilon\}=\begin{Bmatrix}\varepsilon_p^L\\0\end{Bmatrix}+\begin{Bmatrix}z\varepsilon_b\\\varepsilon_s\end{Bmatrix}+\begin{Bmatrix}\varepsilon_p^{\mathrm{NL}}\\0\end{Bmatrix} \tag{9}$$

where the membrane strains $\{\varepsilon_p^L\}$, bending strains $\{\varepsilon_b\}$, shear strains $\{\varepsilon_s\}$, and nonlinear in-plane strains $\{\varepsilon_p^{\mathrm{NL}}\}$ in Eq. (9) are written as [16]

$$\{\varepsilon_p^L\}=\begin{Bmatrix}\frac{\partial u_o}{\partial s}+\frac{w}{R}\\ \frac{u_o\sin\phi}{r}+\frac{w\cos\phi}{r}\\ -\frac{v_o\sin\phi}{r}+\frac{\partial v_o}{\partial s}\end{Bmatrix}$$

$$\{\varepsilon_b\}=\begin{Bmatrix}\frac{\partial\beta_s}{\partial s}+\frac{\partial u_o}{R\partial s}\\ \frac{\beta_s\sin\phi}{r}+\frac{u_o\sin\phi}{Rr}\\ \frac{\partial v_o}{\partial s}\frac{\cos\phi}{r}+\frac{\partial\beta_\theta}{\partial s}-\frac{\beta_\theta\sin\phi}{r}\end{Bmatrix} \qquad \{\varepsilon_s\}=\begin{Bmatrix}\beta_s+\frac{\partial w}{\partial s}\\ \beta_\theta-\frac{v_o\cos\phi}{r}\end{Bmatrix}$$

$$\{\varepsilon_p^{\mathrm{NL}}\}=\begin{Bmatrix}\frac{1}{2}+\left(\frac{\partial w}{\partial s}\right)^2\\0\\0\end{Bmatrix} \tag{10}$$

where r, R, and ϕ are, respectively, the radius of the parallel circle, the radius of the meridional circle, and the angle made by the tangent at any point in the middle surface of the shell with the axis of revolution.

The potential energy functional U can be written in terms of the field variables u_0, v_0, w_o, β_s, β_θ, and their derivatives. The kinetic energy includes the effects of in-plane and rotary inertia terms. The governing equations obtained using Lagrange's equation of motion are solved based on finite element procedure. Using Eqs. (3–10) and following the procedure outlined in the work of Rajasekaran and Murray [17], the finite element equations thus derived are

$$[M]\{\ddot{\boldsymbol{\delta}}\}+([K]+\tfrac{1}{2}N_1(\boldsymbol{\delta})]+\tfrac{1}{3}[N_2(\boldsymbol{\delta})])\{\boldsymbol{\delta}\}=\{\boldsymbol{F}\} \tag{11}$$

where $[K]$ and $[M]$ are the linear stiffness and mass matrices, respectively; $[N_1]$ and $[N_2]$ are nonlinear stiffness matrices that are, respectively, linearly and quadratically dependent on the field variables; $\{\boldsymbol{F}\}$ is the load vector, consisting of mechanical load $\{F_M\}$ and thermal load $\{F_T\}$; and $\{\ddot{\boldsymbol{\delta}}\}$ and $\{\delta\}$ are the acceleration and displacement vectors, respectively. The three-noded finite element employed here has five degrees of freedom $(u_0, v_0, w_o, \beta_s, \beta_\theta)$ per node. The resulting nonlinear Eq. (11) is solved for dynamic response histories employing Newmark's numerical integration method coupled with Newton–Raphson iteration. The dynamic buckling loads are evaluated based on the displacement response histories.

The criterion suggested by Budiansky and Roth [2] is employed here, because it is widely accepted. This criterion is based on the plots of the peak nondimensional average displacement in the time history of the structure with respect to the amplitude of the thermal load. There is a temperature difference range at which a sharp jump in peak average displacement occurs for a small change in load magnitude. The temperature load that corresponds to the inflection point of the load-deflection curve is considered to be the dynamic buckling temperature difference.

III. Results and Discussion

In this section, we use the preceding formulation to investigate the effect of parameters such as gradient index, geometric shell parameter, and boundary condition on the dynamic buckling temperature of functionally graded spherical caps. Because the finite element used here is based on the field-consistency approach, an exact integration is employed to evaluate all the strain energy terms. The shear correction factor, which is required in a first-order theory to account for the variation of transverse shear stresses, is taken as $5/6$. For the present analysis, based on progressive mesh refinement, 15-element idealization is found to be adequate for modeling the spherical caps. For the sake of brevity, these studies are not reported here.

The FGM spherical shell considered here consists of aluminum and alumina. Young's modulus, the conductivity, and the coefficient of thermal expansion for alumina are [18] $E_c=380$ GPa, $\kappa_c=10.4$ W/mK, and $\alpha_c=7.4\times10^{-6}$ (1/°C), respectively, whereas for aluminum, these are $E_m=70$ GPa, $\kappa_m=204$ W/mK, and $\alpha_m=23\times10^{-6}$ (1/°C), respectively. The spherical shell is of uniform thickness and boundary conditions considered here are, for simply supported,

$$u=v=w=0; \qquad \beta_r\neq\beta_\theta\neq0 \qquad \text{on } r=a$$

and for clamped supported,

$$u=v=w=\beta_s=\beta_\theta=0 \qquad \text{on } r=a$$

where a is the base radius.

Before proceeding to the dynamic thermal buckling characteristics of FGM cases, the efficacy of the formulation is tested for the problems for which the analytical solutions are available in the literature [4,19,20]. Table 1 shows the linear critical thermal buckling strain pertaining to simply supported isotropic hemispherical shells, along with those of [19,20]. The nonlinear formulation developed herein is also examined for clamped isotropic $(k=0)$ spherical caps subjected to uniform external pressure of infinite duration, and the results are shown in Fig. 1, along with those of [4], for different values of the geometrical parameter $\lambda=2[3(1-\nu^2)]^{1/4}(H/h)^{1/2}$, where H is the central shell rise. It is inferred that the present results are in very good agreement with the analytical solutions.

Next, the results for nonlinear dynamic thermal buckling analysis of functionally graded spherical caps is presented in terms of critical bucking temperature difference $\Delta T_{\mathrm{cr}}(=T_c-T_m)$. For the chosen shell parameter and power-law index of FGM, the thermal buckling study is conducted for suddenly applied temperature load. The length of response calculation time

Table 1 Comparison of the critical thermal buckling strain ε_T for simply supported isotropic hemispherical shells

h/R	Eslami et al. [19]	Ganesan and Ravikiran [20]	Present
0.01	0.00413	0.00407	0.00424
0.02	0.00844	0.00844	0.00840
0.03	0.01120	0.01204	0.01251
0.04	0.01726	0.01624	0.01657
0.05	0.02149	0.02034	0.02052
0.06	0.02614	0.02379	0.02446
0.07	0.03162	0.02764	0.02844
0.08	0.03574	0.03164	0.03222
0.09	0.03991	0.03530	0.03584
0.10	0.04457	0.03927	0.03944

$$\tau\left(=\sqrt{\frac{E_{\mathrm{ef}}h^2}{12(1-\nu^2)\rho_{\mathrm{ef}}a^4}}t\right)$$

in the present study is varied between one and two, with the criterion that in the neighborhood of the buckling, τ is large enough to allow deflection-time curves to develop fully. $E_{\mathrm{ef}} = (1/2)\int_{-h/2}^{h/2} E(z)\,\mathrm{d}z$ corresponds to the effective modulus of the corresponding gradient index. The time step selected, based on the convergence study, is $\delta t = 0.002$. The values selected for τ and $\delta\tau$ are of the same order as that available in the literature [21,22].

The detailed investigation for dynamic buckling of clamped functionally graded spherical caps is carried out for different geometrical parameters and material power-law indices. A typical nonlinear axisymmetric dynamic response history with time for a clamped isotropic spherical shell parameter ($\lambda = 6$, $a/h = 400$, and $k = 0$) that considers temperature loads is shown in Fig. 2. Further, using such plots, the variation of maximum average displacement with applied temperature obtained is also highlighted as an inset in Fig. 2 for predicting the critical temperature difference. It is seen that there is a sudden jump in the value of the average displacement when the temperature difference reaches the value $\Delta T_{\mathrm{cr}} = 4.7492$ for the shell considered here.

The results evaluated for simply supported FGM spherical caps ($k \neq 0$) are shown in Fig. 3. It is revealed from this figure that with the increase in power-law index k, the critical dynamic buckling temperature difference ΔT decreases, irrespective of shell

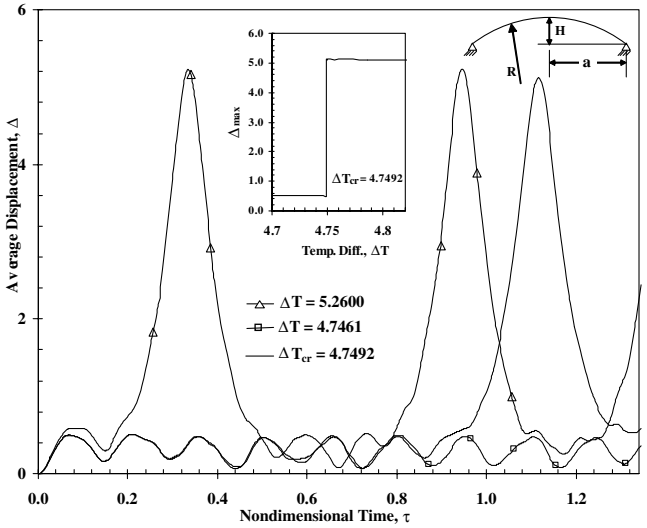

Fig. 2 Average displacement vs nondimensional time for a clamped isotropic spherical cap ($\lambda = 6, k = 0$) under thermal loading.

geometrical parameter. This is attributed to the stiffness reduction because of the increase in the metallic volumetric fraction and the introduction of different stiffness couplings, due to elastic properties variation through the thickness of the FGM shell. It can be also noted that the rate of increase in the critical dynamic buckling temperature difference with respect to the geometrical parameter λ is almost constant for shallow shells, whereas it highly depends on the deep shell geometric parameter value. It can also be noted that the average displacement increases gradually with an increase in temperature load for low values of the geometrical parameter ($\lambda < 5$), indicating the absence of a sudden jump in amplitude with temperature. For the sake of brevity, these studies are not reported here. Such shells may fail due to material failure. A linear static thermal buckling analysis for FGM spherical caps is carried out to compare the nonlinear dynamic thermal buckling behavior. It can be opined that the linear static thermal buckling results (Fig. 4) are significantly higher than the nonlinear dynamic buckling temperature difference. The buckling behavior is qualitatively similar for both cases. However,

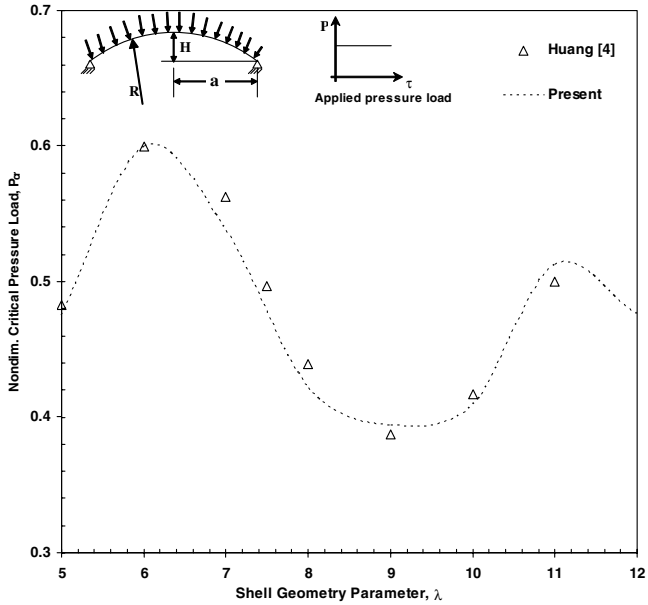

Fig. 1 Comparison of axisymmetric nondimensional critical dynamic pressure P_{cr} for a clamped isotropic ($k = 0$) spherical cap under mechanical loading.

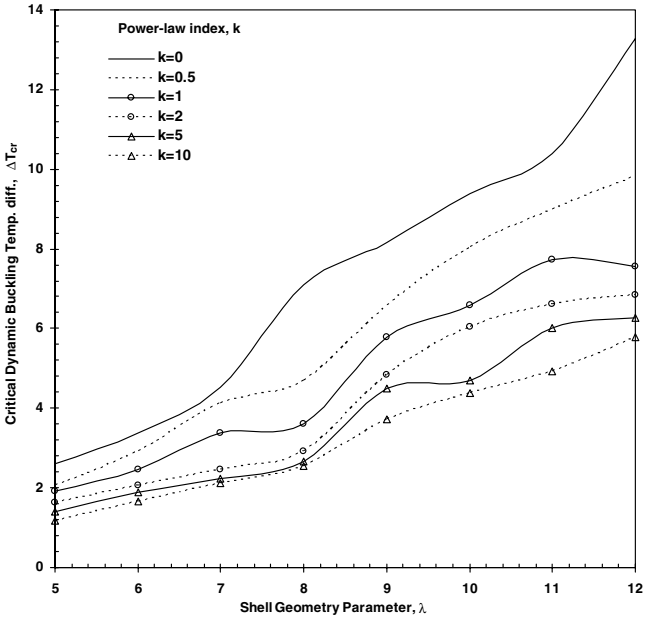

Fig. 3 Variation of the critical dynamic buckling temperature difference against shell geometry parameter λ of simply supported FGM spherical caps.

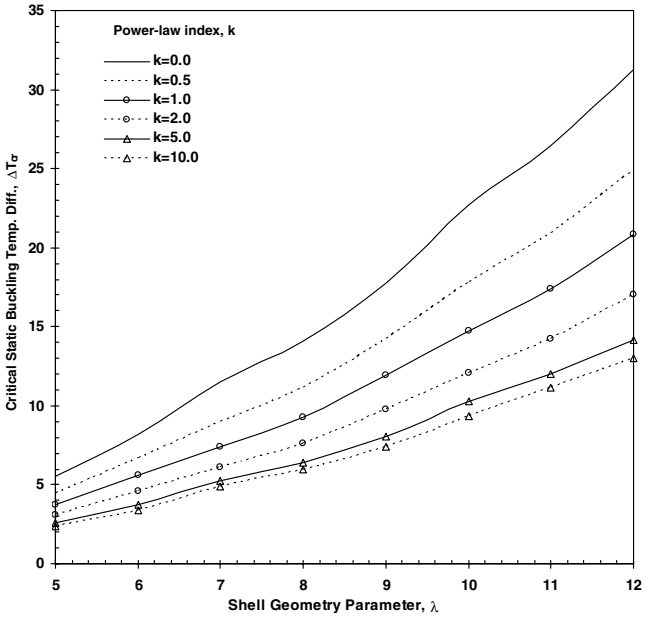

Fig. 4 Variation of the critical static buckling temperature difference against shell geometry parameter λ of simply supported FGM spherical caps.

unlike the nonlinear dynamic analysis case, the critical bucking load monotonically increases with geometric parameters.

IV. Conclusions

Axisymmetric dynamic buckling analysis of functionally graded spherical caps subjected to thermal load has been examined through nonlinear transient dynamic response. A three-noded axisymmetric curved shell element based on field-consistency principle has been employed for this purpose. Numerical results obtained here for an isotropic case that considers pressure load are found to be in good agreement with the previous studies. From the detailed study, it is observed that the critical dynamic buckling temperature difference of a spherical cap decreases with the material power-law index and increases, in general, with the shell geometrical parameters. Furthermore, the influence of deep shell parameters is significant on the critical values. It is hoped that this study will be useful for the designers while optimizing the FGM-based shell structures exposed to thermal environment.

References

[1] Koizumi, M., "FGM Activities in Japan," *Composites, Part B: Engineering*, Vol. 28, No. 1–2, 1997, pp. 1–4.

[2] Budiansky, B., and Roth, R. S., "Axisymmetric Dynamic Buckling of Clamped Shallow Spherical Shells," NASA TND-510, 1962, pp. 597–609.

[3] Simitses, G. J., "Axisymmetric Dynamic Snap-Through Buckling of Shallow Spherical Caps," *AIAA Journal*, Vol. 5, May 1967, pp. 1019–1021.

[4] Haung, N. C., "Axisymmetric Dynamic Snap-Through of Elastic Clamped Shallow Shell," *AIAA Journal*, Vol. 7, No. 2, 1969, pp. 215–220.

[5] Chao, C. C., and Lin, I. S., "Static and Dynamic Snap-Through of Orthotropic Spherical Caps," *Composite Structures*, Vol. 14, No. 4, 1990, pp. 281–301.

[6] Ganapathi, M., Gupta, S. S., and Patel, B. P., "Nonlinear Axisymmetric Dynamic Buckling of Laminated Angle-Ply Composite Spherical Caps," *Composite Structures*, Vol. 59, No. 1, Jan. 2003, pp. 89–97.

[7] Makino, A., Araki, N., Kitajima, H., and Ohashi, K., "Transient Temperature Response of Functionally Gradient Material Subjected to Partial, Stepwise Heating," *Transactions of the Japan Society of Mechanical Engineers, Series A*, Vol. 60, No. 580, 1994, pp. 222–228.

[8] Obata, Y., and Noda, N., "Steady Thermal Stresses in a Hollow Circular Cylinder and a Hollow Sphere of a Functionally Gradient Material," *Journal of Thermal Stresses*, Vol. 17, No. 3, 1994, pp. 471–487.

[9] Takezono, S., Tao, K., Inamura, E., and Inoue, M., "Thermal Stress and Deformation in Functionally Graded Material Shells of Revolution Under Thermal Loading Due to Fluid," *JSME International Journal, Series A: Mechanics and Material Engineering*, , Vol. 39, No. 4, 1994, pp. 573–581.

[10] Ng, T. Y., Lam, K. Y., Liew, K. M., and Reddy, N. J., "Dynamic Stability Analysis of Functionally Graded Cylindrical Shells Under Periodic Axial Loading," *International Journal of Solids and Structures*, Vol. 38, No. 8, 2001, pp. 1295–1309.

[11] Loy, C. T., Lam, K. Y., and Reddy, J. N., "Vibration of Functionally Graded Cylindrical Shells," *International Journal of Mechanical Sciences*, Vol. 41, No. 3, 1999, pp. 309–324.

[12] Simitses, G. J., *Dynamic Stability of Suddenly Loaded Structures*, Springer–Verlag, New York, 1989.

[13] Mori, T., Tanaka, K., "Average Stress in Matrix and Average Elastic Energy of Materials with Misfitting Inclusions," *Acta Metallurgica*, Vol. 21, No. 5, 1973, pp. 571–574.

[14] Benveniste, Y., "A New Approach to the Application of Mori–Tanaka's Theory in Composite Materials," *Mechanics of Materials*, Vol. 6, No. 2, 1987, pp. 147–157.

[15] Qian, L. F., Batra, R. C., and Chen, L. M., "Static and Dynamic Deformations of Thick Functionally Graded Elastic Plates by Using Higher-Order Shear and Normal Deformable Plate Theory and Meshless Local Petrov-Galerkin Method," *Composites, Part B: Engineering*, Vol. 35, Nos. 6–8, 2004, pp. 685–697.

[16] Kraus, H., *Thin Elastic Shells*, Wiley, New York, 1967.

[17] Rajasekaran, S., and Murray, D. W., "Incremental Finite Element Matrices," *Journal of the Structural Division*, Vol. 99, No. 12, 1973, pp. 2423–2438.

[18] Lanhe, Wu., "Thermal Buckling of a Simply Supported Moderately Thick Rectangular FGM Plate," *Composite Structures*, Vol. 64, No. 2, 2004, pp. 211–218.

[19] Eslami, M. R., Ghorbani, H. R., and Shakeri, M., "Thermoelastic Buckling of Thin Spherical Shells," *Journal of Thermal Stresses*, Vol. 24, No. 12, 2001, pp. 1177–1198.

[20] Ganesan, N., and Ravikiran K., "A Theoretical Analysis of Linear Thermoelastic Buckling of Composite Hemispherical Shells with a Cut-Out at the Apex," *Composite Structures*, Vol. 68, No. 1, 2005, pp. 87–101.

[21] Ball, R. E., and Burt, J. A., "Dynamic Buckling of Shallow Spherical Shells," *Journal of Applied Mechanics*, Vol. 40, June 1973, pp. 411–416.

[22] Kao, R., "Nonlinear Dynamic Buckling of Spherical Caps with Initial Imperfection," *Computers and Structures*, Vol. 12, July 1980, pp. 49–63.

S. Saigal
Associate Editor